Size dependence of tetrahedral bond lengths in CdSe nanocrystals

Pin-Jiun Wu, Yuri P. Stetsko, Ku-Ding Tsuei, Roman Dronyak, and Keng S. Liang

Citation: Applied Physics Letters **90**, 161911 (2007); doi: 10.1063/1.2727559
View online: http://dx.doi.org/10.1063/1.2727559
View Table of Contents: http://scitation.aip.org/content/aip/journal/apl/90/16?ver=pdfcov
Published by the AIP Publishing

Size dependence of tetrahedral bond lengths in CdSe nanocrystals

Pin-Jiun Wu
Department of Electrophysics, National Chiao Tung University, Hsinchu 300, Taiwan and National Synchrotron Radiation Research Center, Hsinchu 300, Taiwan

Yuri P. Stetsko, Ku-Ding Tsuei, and Roman Dronyak
National Synchrotron Radiation Research Center, Hsinchu 300, Taiwan

Keng S. Liang[a)]
National Synchrotron Radiation Research Center, Hsinchu 300, Taiwan and Department of Electrophysics, National Chiao Tung University, Hsinchu 300, Taiwan

(Received 1 December 2006; accepted 20 March 2007; published online 18 April 2007)

The structural characteristics of organically passivated CdSe nanocrystals (NCs) were investigated with x-ray diffraction and extended x-ray absorption fine structure. As the NC size decreases, the axial bond length $R^{(1)}$ for an atomic tetrahedron extends but the equatorial bond length $R^{(2)}$ contracts, with a similar tendency of distortion for the lattice parameters of the wurtzite structure. The authors suggest that the observed hexagonal distortion is attributed to the surface stress of the NCs related to the organic passivation effect and the relaxation of atomic positions at the stacking fault interface. © *2007 American Institute of Physics*. [DOI: 10.1063/1.2727559]

Extensively applied in biosensors, solar cells, and light-emitting diodes, CdSe nanocrystals (NCs) attract wide interest.[1] Their tunable merits in physical and chemical properties particularly focus attention on many unresolved problems. The stable, controllable, and monodispersed NCs offer an opportunity to explore the dimensionally dependent characteristics of materials, involving structural dynamics, surface effects, and optical performance.[2] These various properties of NCs have thus warranted continuous research. X-ray diffraction (XRD) and extended x-ray absorption fine structure (EXAFS) spectroscopy are powerful tools to study the crystallite structure of nanomaterials.[3] In contrast with some local probes such as transmission electron microscopy or atomic-force microscopy, XRD and EXAFS spectra can provide more quantitative information on the internal structure. With progress in the preparation of small clusters, NCs of a high quality and narrow distribution of size provide an opportunity to investigate the size-dependent properties of materials using large-area probing tools. We here report the observation of a nonuniform distortion of a tetrahedral structure in CdSe NCs with respect to their size.

Organically stabilized CdSe NCs were prepared according to an organometallic synthesis in an environment free of air, using trioctylphosphine oxide (TOPO) and hexadecylamine (HDA) as the surface passivants.[4,5] By controlling the duration of reaction and the conditions of growth, CdSe NCs of varied sizes (D) can be obtained. The size distribution of NCs thus prepared has about 5% standard deviation, as verified with a transmission electron microscope (TEM) and optical spectra.

XRD data were collected on a diffractometer operated in the Bragg configuration using 8 keV x rays. The NC powder samples for diffraction measurements were obtained by drop casting the dispersion of CdSe NCs with toluene on a silicon wafer and then slowly evaporating the solvent. The silicon substrate was chosen to decrease the x-ray scattering background. Figure 1 shows XRD data for CdSe NCs and the corresponding patterns calculated with a discrete form of the Debye formula including a Debye-Waller (DW) factor.[6] In our calculations we took into account the nearly spherical shape of particles, the lattice distortion, the surface disorder, and the layer-stacking sequences (polytypic structure).[7] The observed broadening of the diffraction features is due primarily to the diminished size of NC domains, but surface reconstruction causes further broadening.[7] All peaks have a slight shift dependent on the particle size, indicating the presence of a lattice distortion.

Both the wurtzite (W) and zinc blende (ZB) structures are based on the stacking of identical two-dimensional planar

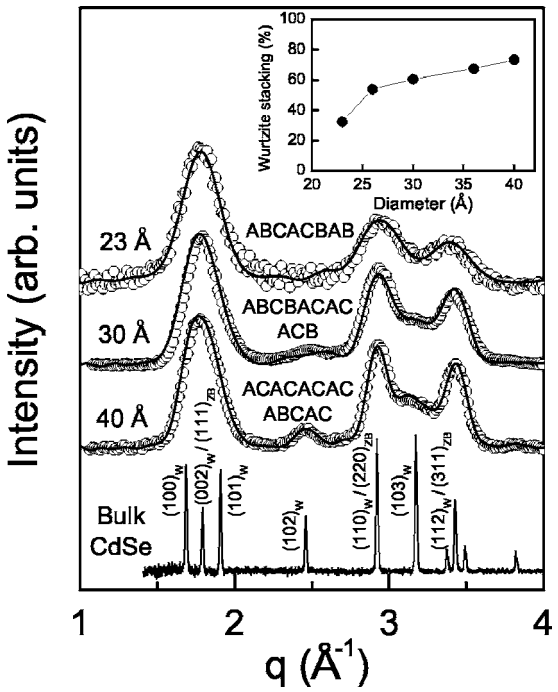

FIG. 1. Powder diffraction data (symbols) and calculated patterns (lines) for CdSe NCs, as well as the layer-stacking sequences. Inset: the wurtzite stacking fraction (in percent) as a function of the NC diameter.

[a)]Author to whom correspondence should be addressed; electronic mail: ksliang@nsrrc.org.tw

units translated with respect to each other, in which each atom is tetrahedrally surrounded with four nearest neighbors. The layer stacking is described as $ABABAB\cdots$ along the [001] axis for W and as $ABCABC\cdots$ along the [111] axis for ZB. We use the polytypic structures composed of W and ZB layer stackings to obtain acceptable fits of the experimental data. These sequences represent the presence of several stacking faults in the W (or ZB) structure that have been observed also with TEM.[4] The inset of Fig. 1 reveals that the layer stacking of W increases with increasing particle size, which is accompanied by some enhanced features that appear only for the W structure [see, for example, the $(102)_W$ and $(103)_W$ reflections in Fig. 1]. The stacking sequences indicated in Fig. 1 are not unique: similarly satisfactory fits of the experimental data can be achieved for other stacking sequences, which, nevertheless, yield similar values of W stacking fractions in NCs.

The observed phase transition depending on the cluster size can be described by a thermodynamic model.[8] For bulk CdSe, the critical temperature T_c of the ZB-to-W structural phase transition is about 95 °C,[9] indicating that for as-prepared CdSe NCs the chemical potential $\mu^0_{ZB} > \mu^0_W$ at the growth temperature (~270 °C). However, CdSe NCs with very small size possess a ZB structure at any temperature of preparation.[4,10] Considering the chemical/mechanical potential $g^* = \mu^0 + 6f\bar{V}/D$,[11] we should assume $f_{ZB} < f_W$ to satisfy the experimental results ($g^*_{ZB} < g^*_W$ for small cluster), where f is the surface free energy and $\bar{V}$ is the partial molar volume of the constituent of the grain.[8] With the particle size increasing, therefore, there would be a possibility of the phase transition from a ZB to a W structure, consistent with our observation in the inset of Fig. 1.

With synchrotron radiation, EXAFS spectra were collected in the fluorescence mode on samples at a temperature of ~10 K. Bulk CdSe that served as the reference was measured under conditions similar to those for the NCs, which was used to determine the reduction factor S_0^2 and threshold energy E_0. To analyze the EXAFS data, we followed standard procedures, including preedge and postedge background subtraction, normalization with respect to the edge jump, Fourier transformation, and curve fitting. All computer programs were implemented in the UWXAFS 3.0 package. The phase shift and backscattering amplitude functions for specific atom pairs were calculated *ab initio* with the FEFF6 code.

For a real W system, bonds between nearest-neighbor anion and cation for a tetrahedral structure have two distinct lengths. The length of the axial bond, along the c axis, is defined as $R^{(1)} = uc$; three other bonds have equal length $R^{(2)} = a\sqrt{1/3 + (1/2-u)^2 (c/a)^2}$, in which u denotes the dimensionless internal-cell structural parameter.[12] In an ideal W structure for which $c/a = \sqrt{8/3}$ and $u = 3/8$, the bond lengths are equal $[R^{(1)} = R^{(2)}]$. We used the above expressions with lattice parameters obtained from the fit of XRD data and applied a restriction on the coordination number $3N_{R^{(1)}} = N_{R^{(2)}}$ to fit all Se K-edge EXAFS spectra; in addition, the DW factors of these two bond lengths were constrained to be the same.

Figure 2 shows the first-shell filtered data of $\chi(k)^* k$ of three NCs and a bulk sample together with the corresponding fits. Satisfactory fits with only Cd backscatter were achieved, indicating that Se has only Cd as its nearest-neighboring atoms. Of three qualitative trends that we observed, the progressive increase of the oscillation period indicates that the mean Cd–Se bond length contracts with decreasing particle size, which is accompanied by a broadening due to larger structural disorder; the variation of Se K-edge spectral amplitude among samples is less noticeable, reflecting that most Se atoms are located in the interior of NC, and all spectra seem to be composed of oscillations with a single frequency, indicating that EXAFS is dominated by the contribution from the first coordination shell. The Cd K-edge EXAFS data were also analyzed (not shown here); since the surface Cd atom has not only Se but also O and/or N as its nearest neighbors, this report focuses on Se K-edge EXAFS from Cd–Se pairs to prevent the unnecessary fitting deviation.

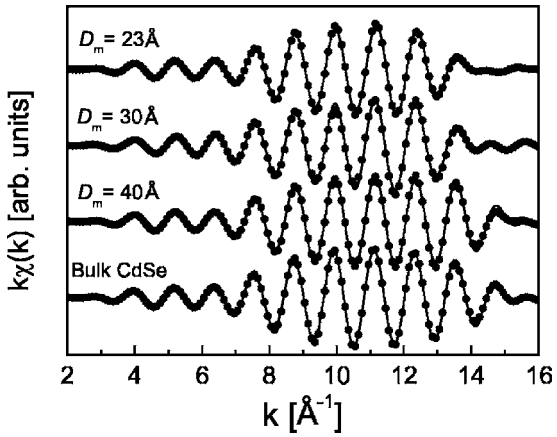

FIG. 2. Single-shell filtered Se K-edge data (symbols) and the corresponding fits (lines). The NC and bulk CdSe data were filtered over an identical range of 1.5–3.3 Å in r space.

The lattice parameters c_{NC} and a_{NC} normalized to those of bulk CdSe, presented in Fig. 3, are obtained from fits of the diffraction patterns of CdSe NCs. For bulk CdSe, the lattice parameters are $c_b = 7.01$ Å and $a_b = 4.299$ Å. Our results show that a decreasing particle size is correlated with an expansion in c_{NC} and a contraction in a_{NC} relative to bulk values, indicating a nonuniform distortion of the unit cell, as also found for CdS particles.[13] The distinct bond lengths $R^{(1)}_{NC}$ and $R^{(2)}_{NC}$ normalized to those of bulk CdSe obtained from the fit of the Se K-edge EXAFS data are plotted in Fig. 3, with lattice parameters for comparison. A schematic diagram of an

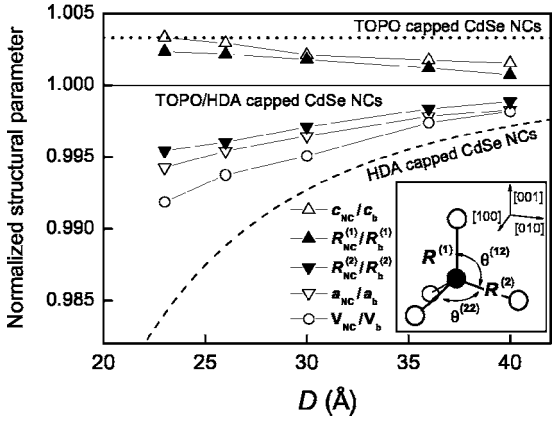

FIG. 3. Size dependence of structural parameters for CdSe NCs. The dotted and dashed lines represent the normalized lattice parameter as a function of particle size for CdSe NCs passivated with TOPO and HDA (deduced from Ref. 15), respectively. Inset: the scheme of a tetrahedral structure.

atomic tetrahedron is shown in the inset. $R^{(1)}$ has a tendency to expand whereas $R^{(2)}$ exhibits a contraction as NCs become smaller. $R_{\mathrm{NC}}^{(1)}/R_b^{(1)}$ and $R_{\mathrm{NC}}^{(2)}/R_b^{(2)}$ show a size dependence similar to c_{NC}/c_b and a_{NC}/a_b, respectively. This observation implies that the structural parameter u remains almost constant even for small NCs. According to the variations of $R^{(1)}$ and $R^{(2)}$, the axial bond angle $\theta^{(12)}$ of a tetrahedral structure (see the inset of Fig. 3) becomes larger with decreasing size, whereas the equatorial bond angle $\theta^{(22)}$ reveals an opposite behavior. The structural distortion and, in particular, the decreased volume of the unit cell of NCs are attributed to an increased ratio of surface to volume with decreasing NC size.

The change in lattice parameter of a spherical cluster compared to that of the bulk can be related to the surface stress through the concept of the surface pressure, following the modified Laplace law for solids:[3,8] $P=4\Gamma_s/D=E/(1-2\nu)[(a_{\mathrm{NC}}-a_b)/a_{\mathrm{NC}}]$, where Γ_s is surface stress, E is the Young modulus [41.5 GPa for CdSe (Ref. 14)], and ν is the Poisson coefficient [0.37 for CdSe (Ref. 14)]. Meulenberg *et al.*[15] reported that the measured stress of CdSe NCs, using resonance Raman spectroscopy, is related to surface passivation: CdSe NCs passivated with HDA show the size-dependent compressive stress, which leads to contraction of lattice; for CdSe NCs passivated with TOPO, on the other hand, the results exhibit tensile stress giving rise to lattice expansion and do not follow a smooth functional relationship ($P\approx-0.53$ GPa in average). Accordingly, the variations of the lattice with size for CdSe NCs passivated with HDA and TOPO are plotted in Fig. 3 as dashed and dotted lines, respectively. The size-dependent $R_{\mathrm{NC}}^{(2)}/R_b^{(2)}$ and a_{NC}/a_b apparently reveal some combined effects of stress from TOPO and HDA surfactants, consistent with our EXAFS results (the surface Cd atoms attached to TOPO/HDA), with a net decrease. According to the modified Laplace law, the continuous decrease in a_{NC} with decreasing NC size reflects the increasing surface pressure and surface stress.

The surface energy deduced from the change in the lattice parameter[3] approaches zero for all NC samples. This is due to the effect of surface passivation or adsorption on the thermodynamic behavior for small particles being to reduce the surface energy.[3] In addition, an increasing fraction of ZB stacking via stacking faults, with decreasing particle size, can also lower the surface energy, owing to $f_{\mathrm{ZB}}<f_{\mathrm{W}}$ for CdSe, as discussed above.

Different from $R_{\mathrm{NC}}^{(2)}$ and a_{NC}, however, $R_{\mathrm{NC}}^{(1)}$ and c_{NC} become expanded compared to bulk CdSe (R_b). The relaxation of the atomic positions at a stacking fault interface can result in an increase of the bond length normal to the fault plane, which was reported for bulk AlN and GaN using *ab initio* calculations.[16] As shown in Fig. 1, moreover, the small NCs possess the higher density of stacking fault. The observed expansion in $R_{\mathrm{NC}}^{(1)}$ and c_{NC} of CdSe NCs may be induced by two competing effects of surface reconstruction driven by surface stress and atomic relaxation due to stacking faults. We note that, nevertheless, the overall effect of the surface pressure or stress is still compressive, leading to a volume decrease of the unit cell with decreasing size.

In summary, we characterized the structural parameters of organically stabilized CdSe NCs by analyzing XRD and EXAFS spectra. The size-dependent behavior of the distinct tetrahedral bond lengths correlated with wurtzite lattice parameters. The structural distortion of the NCs is explained as due to surface stress depending on the surface passivation and atomic relaxation related to the presence of stacking faults.

The authors thank Jyh-Fu Lee and Kung-Hwa Wei for helpful discussions and Meng-Ting Hsieh and Hang-Chang Chang for providing the NC samples. One of the authors (P.J.W.) thanks Din-Goa Liu, Tu-Li Tai, and Heng-Jui Liu for assistance in the EXAFS and XRD experiments. National Science Council, Taiwan, has supported this work under Grant No. NSC 94-2122-M-213-017.

[1] M. Bruchez, M. Moronne, P. Gin, S. Weiss, and A. P. Alivisatos, Science **281**, 2013 (1998); W. U. Huynh, J. J. Dittmer, and A. P. Alivisatos, *ibid.* **295**, 2425 (2002).
[2] H. Borchert, D. V. Talapin, N. Gaponik, C. McGinley, S. Adam, A. Lobo, T. Moller, and H. Weller, J. Phys. Chem. B **107**, 9662 (2003); C. McGinley, M. Riedler, T. Moller, H. Borchert, S. Haubold, M. Haase, and H. Weller, Phys. Rev. B **65**, 245308 (2002).
[3] Y. Champion, F. Bernard, N. Millot, and P. Perriat, Appl. Phys. Lett. **86**, 231914 (2005).
[4] C. B. Murray, D. J. Norris, and M. G. Bawendi, J. Am. Chem. Soc. **115**, 8706 (1993).
[5] P. Reiss, J. Bleuse, and A. Pron, Nano Lett. **2**, 781 (2002).
[6] A. Guinier, *X-ray Diffraction* (Freeman, San Francisco, 1963), pp. 49–51.
[7] M. G. Bawendi, A. R. Kortan, M. L. Steigerwald, and L. E. Brus, J. Chem. Phys. **91**, 7282 (1989).
[8] P. Perriat and J.-C. Niepce, J. High Temp. Chem. Processes **3**, 585 (1994).
[9] V. A. Fedorov, V. A. Ganshin, and Yu. N. Korkishko, Phys. Status Solidi A **126**, K5 (1991).
[10] R. J. Bandaranayake, G. W. Wen, J. Y. Lin, H. X. Jiang, and C. M. Sorensen, Appl. Phys. Lett. **67**, 831 (1995).
[11] P. Perriat, J. C. Niepce, and G. Caboche, J. Therm. Anal. **41**, 635 (1994).
[12] C. Y. Yeh, Z. W. Lu, S. Froyen, and A. Zunger, Phys. Rev. B **46**, 10086 (1992).
[13] C. Kumpf, R. B. Neder, F. Niederdraenk, P. Luczak, A. Stahl, M. Scheuermann, S. Joshi, S. K. Kulkarni, C. Barglik-Chory, C. Heske, and E. Umbach, J. Chem. Phys. **123**, 224707 (2005).
[14] S. Banerjee, S. Jia, D. I. Kim, R. D. Robinson, J. W. Kysar, J. Bevk, and I. P. Herman, Nano Lett. **6**, 175 (2006).
[15] R. W. Meulenberg, T. Jennings, and G. F. Strouse, Phys. Rev. B **70**, 235311 (2004).
[16] J. A. Majewski and P. Vogl, MRS Internet J. Nitride Semicond. Res. **3**, 21 (1998).